The following supplement accompanies the article

A fully coupled ecosystem model to predict the foraging ecology of apex predators in the California Current

J. Fiechter*, L. A. Huckstadt, K. A. Rose, D. P. Costa

*Corresponding author: fiechter@ucsc.edu

Marine Ecology Progress Series 556: 273–285 (2016)

1. Bioenergetics for California Sea Lions IBM

Bioenergetics of each sea lion individual is represented by a mechanistic dynamic model based on the formulation proposed by Lavigne et al. (1982), which separates the energy demands of an animal between two main components: production (somatic and reproductive growth) and maintenance (resting metabolism, activity and work, cost of digestion). Since the costs associated with reproductive growth can be neglected for male mammals, the bioenergetics model is simplified to:

Production = Consumption - Metabolism - Waste

Depending on the daily balance between energy acquired from consumption and the energy required for production and metabolism, three different conditions are considered: optimal growth, sub-optimal growth, and negative growth. Under optimal growth conditions, the animal acquired sufficient energy to meet the desired daily growth and any excess energy is therefore allocated to fat depot. Under sub-optimal growth conditions, the energy balance is positive, but not sufficient to achieve desired growth, and the animal uses the energy to maintain homeostasis and the desired protein to fat ratio, instead of realizing the desired growth. Under negative growth conditions, the animal does not acquire enough energy to fulfill its energetic demands, and fat and protein are catabolized to satisfy energy requirements, affecting the desired protein to fat proportion. Loss of the individual (i.e., starvation) is assumed when the dynamically-adjusted fat component falls below 5% of body mass. Since the sea lion bioenergetics component is solved hourly, daily consumption and metabolic rates are scaled to hourly values through multiplication by the model time step (Δt = 1 hour). Bioenergetics results in production, which determines the body mass (W in kg) of each individual. From hourly values of production and body mass, additional individual traits are computed, such as protein and mass fractions of body mass, length, physiological age, and diet composition.

1.1 Consumption

Sea lion energy consumption is calculated for each hourly time step using an estimate of daily food consumption (in units of biomass) based on its relationship to body mass (W):

$$C_{max}[kg] = 0.115 \cdot W \cdot \Delta t$$

The body mass coefficient was adjusted to 11.5% from its original value of 9% (Kastelein et al. 2000) to reflect observed energy demand identified based on tracking data for male sea lion off of central California. The model assumes that sea lions preferentially feed on Pacific sardine and northern anchovy (from the forage fish component of the IBM), but also have access to other resources (market squid and jack mackerel) to meet part of their daily energy requirement. These four prey items are included in the model based on long-term diet data for California sea lions (Lowry and Carretta 1999), as well as based on the availability of information on their energetic densities (Glaser 2010) and on prey-specific assimilation efficiencies of the sea lions (Costa 1986). For sardine and anchovy, sea lions dynamically feed on fish individuals located within swimming distance on the ROMS grid. At each time step, available biomass (B) of sardine and anchovy are weighted by species-specific vulnerability (υ) and feeding efficiency (K) parameters (Table 1), and combined into a functional response (Rose et al. 1999) that determines sea lion consumption of anchovy (C_A) and sardine (C_S):

$$C_A[kg] = \frac{C_{max} \cdot \left(\frac{B_A \upsilon_A}{K_A}\right)}{1 + \frac{B_A \upsilon_A}{K_A} + \frac{B_S \upsilon_S}{K_S}} \quad and \quad C_S[kg] = \frac{C_{max} \cdot \left(\frac{B_S \upsilon_S}{K_S}\right)}{1 + \frac{B_A \upsilon_A}{K_A} + \frac{B_S \upsilon_S}{K_S}}$$

Although diving behavior is currently neglected in the model (i.e., sea lions only move horizontally on the grid), sea lions are allowed to eat sardine and anchovy individuals located over the entire water column. The feeding efficiency values were calibrated to obtain mean relative diet contributions of roughly 30% for anchovy and 20% for sardine.

During each time step, sea lions are allowed to consume a combined sardine and anchovy biomass up to the hourly fraction of their daily food requirement (i.e., maximum daily consumption multiplied by the model time step). If an individual is unable to meet its desired hourly consumption from sardine and anchovy alone, then the individual can complete the missing prey biomass by feeding on market squid and mackerel. The energy acquired from prey consumption is therefore given by:

$$E_C\ [MJ] = \sum_{i=1}^{4} \propto_i \cdot E_{C,i} \cdot C_{max}$$

where $\propto_i$ and $E_{C,i}$ are the diet fraction and energy density for each prey type (i.e., anchovy, sardine, market squid, and mackerel) (Table 1). The species-specific values for $\propto$ vary dynamically at each time step and for each sea lion individual as a function of the anchovy and sardine biomass encountered and consumed (C_A and C_S), namely:

$$\alpha_{anchovy} = \frac{C_A}{C_{max}}\ ,\ \ \alpha_{sardine} = \frac{C_S}{C_{max}}$$

$$\alpha_{squid} = \varphi \cdot \max\left(1 - (\alpha_A + \alpha_B), 0\right)$$

$$\alpha_{mackerel} = (1 - \varphi) \cdot \max\left(1 - (\alpha_A + \alpha_B), 0\right)$$

where φ accounts for the available market squid biomass relative to that of mackerel. The value of φ is set to 0.77 to reflect the 1989-2008 mean biomasses of market squid and mackerel from California landings data (PFMC 2014) (Fig. S5). Based on the calibration of feeding efficiency and catch information, the average apportion of each prey species consumed by sea lions in the model is approximately 33% for anchovy, 18% for sardine, 38% for market squid, and 11% for mackerel.

1.2 Metabolism and waste

Resting metabolic rate (RMR) is directly related to body mass, while at-sea field metabolic rate (FMR) is based on the animal swimming speed (Feldkamp 1987):

$$RMR\ [MJ] = 0.0864 \cdot 3.4 \cdot W^{0.75} \cdot \Delta t$$

$$FMR\ [MJ\ ] = 0.0864 \cdot 2.1 \cdot e^{0.48*U} \cdot W \cdot \Delta t$$

where U is the swimming speed. The cost of digestion is estimated as the Heat Increment of Feeding (HIF), which corresponds to 12.5% of the energy acquired as food (E_C), and energy losses from excretion (E_W) are summed over each prey source in the diet:

$$E_W\,[MJ] = \sum_{i=1}^{4} \propto_i \cdot \omega_i \cdot E_C$$

where $\propto_i$ is the diet fraction and ω_i is the fractional energy loss associated with each prey type (Table 1). Since California sea lions do not acquire food and have no metabolic costs associated with movement or digestion when hauled out, the metabolic cost during periods spent on land (i.e., when sea lions are often resting or sleeping) is calculated by multiplying the resting rate by a factor of 1.2. RMR plus FMR determines metabolism, and HIF plus E_W determines energy lost due to waste.

1.3 Production

The model calculates the desired growth in length (L) of a sea lion based on a length-age (i.e., von Bertalanffy) relationship:

$$L[cm] = 278.6571 \cdot \left(1 - e^{-0.0882(t+4.6688)}\right)$$

where t is the physiological age in days updated at each hourly time step. The desired increase in length (ΔL) is converted to mass using an allometric relationship derived from field data on male sea lions from central California:

$$dW[kg] = 1.592 \cdot 10^{-5} \cdot L^{2.268} \cdot \Delta L$$

For simplicity, any changes in body mass are ultimately due to changes in the fat and protein fractions, and excess energy is allocated to fat depot. Changes in mass are converted to energetic demands based on tissue-specific energetic efficiency of deposition, energy density of each tissue, as well as targeted body proportions of fat and protein in California sea lions (protein: 26.7% of body mass; fat: 15% of body mass). Considering that the net energy gain available for production at each time step is given by:

$$E_R[MJ] = E_C - [RMR + FMR + HIF + E_W]$$

The corresponding changes in body mass for positive and negative energy gains are (Blaxter 1989; Rea et al. 2007):

$$dB[kg] = \frac{E_R}{\rho_{fat}E_{fat} + \rho_{prot}E_{prot}} \qquad for\ \ E_R > 0$$

$$dB[kg] = E_R\left[\frac{\gamma_{fat}}{\eta_{fat}E_{fat}} + \frac{1-\gamma_{fat}}{\eta_{prot}E_{prot}}\right] \qquad for\ \ E_R < 0$$

where $E_{fat/prot}$ is the production energy for fat/protein, $\rho_{fat/prot}$ is the target body mass fraction for fat/protein, $\eta_{fat/prot}$ is deposition efficiency for fat/protein, and γ_{fat} is the energy fraction derived from fat (Table 1). For positive growth (i.e., $dB > 0$), the following two cases are considered: (1) optimal growth (i.e., $dB > dW$) where excess energy is allocated to fat depot after protein energy requirements are met, and (2) sub-optimal growth (i.e., $dB < dW$) where the net energy gain is use to maintain the targeted protein-to-fat ratio in body mass. For sub-optimal growth, the physiological age and length of the animal are only partially incremented to reflect actual growth given the available energy. For negative growth (i.e., $dB < 0$), both fat and protein mass are lost, with fat depot contributing to ~83% (i.e., γ_{fat}) of the energy demand (Rea et al. 2007). For negative growth, the physiological age and length of the animal remain unchanged from the previous time step. Starvation (i.e., loss of the individual) is assumed when the dynamically-adjusted fat component falls below 5% of body mass.

References

Blaxter, K. L. (1989). *Energy metabolism in animals and man*. CUP Archive.

Costa, D.P., 1986. Assessment of the impact of the California sea lion and the northern elephant seal on commercial fisheries. In: Final Report for California Sea Grant. Biennial Report of Completed Projects 1984-1986. Calif. Sea Grant College Prog., Univ. of California, La Jolla, CA. Publ. No. R-CSGCP-024. pp. 36-43.

Feldkamp, S.D., 1987. Swimming in the California sea lion: morphometrics, drag and energetics. Journal of Experimental Biology 131(1), 117-135.

Glaser, S.M., 2010. Interdecadal variability in predator-prey interactions of juvenile North Pacific albacore in the California Current System. Marine Ecology Progress Series 414, 209-221.

Kastelein, R.A., Schooneman, N.M., Vaughan, N., Wiepkema, P.R., 2000. Food consumption and growth of California sea lions (Zalophus californianus californianus). Zoo Biology 19(2), 143-159.

Lavigne, D.M., Innes, S., Worthy, G.A.J., Kovacs, K.M., 1986. Metabolic rate—body size relations in marine mammals. Journal of theoretical biology 122(1), 123-124.

Pacific Fisheries Management Council (PFMC), 2014. Status of the Pacific coast coastal pelagic species fishery and recommended acceptable biological catches. Stock assessment and fishery evaluation for 2014.

Rea, L.D., Rosen, D.A.S., Trites, A.W., 2007. Utilization of stored energy reserves during fasting varies by age and season in Steller sea lions. Canadian Journal of Zoology 85(2), 190-200.

Rose, K.A., Rutherford, E.S., McDermott, D., Forney, J.L., Mills, E.L., 1999. Individual-based model of walleye and yellow perch populations in Oneida Lake. Ecological Monographs 69, 127-154.

Weise, M.J. and J.T. Harvey, 2008. Temporal variability in ocean climate and California sea lion diet and biomass consumption: implications for fisheries management. Marine Ecology Progress Series 373, 157-172, doi:10.3354/meps07737.

Tables

Table S1. Parameter names, symbols, values, and units for the California sea lion bioenergetics model (nd = non-dimensional). References for parameter values: [1]this study, [2]Glaser 2010, [3]Costa 1986, [4]Blaxter 1989, [5]Rea et al. 2007.

Parameter Name	Symbol	Value	Units
Consumption			
maximum consumption[1]	C	0.115	kg_{prey} kg^{-1} day^{-1}
energy density for anchovy[2]	$E_{anchovy}$	6.6	MJ kg^{-1}
energy density for sardine[2]	$E_{sardine}$	7.3	MJ kg^{-1}
energy density for squid[2]	E_{squid}	4.4	MJ kg^{-1}
energy density for mackerel[2]	$E_{mackerel}$	6.4	MJ kg^{-1}
vulnerability for anchovy[1]	$\nu_{anchovy}$	1.0	nd
vulnerability for sardine[1]	$\nu_{sardine}$	1.0	nd
feeding efficiency for anchovy[1]	$K_{anchovy}$	$5.0 \cdot 10^4$	kg
feeding efficiency for sardine[1]	$K_{sardine}$	$2.0 \cdot 10^3$	kg
Metabolism			
fractional energy loss for anchovy[3]	$\omega_{anchovy}$	0.084	nd
fractional energy loss for sardine[3]	$\omega_{anchovy}$	0.118	nd
fractional energy loss for squid[3]	$\omega_{anchovy}$	0.217	nd
fractional energy loss for mackerel[3]	$\omega_{anchovy}$	0.086	nd
swimming speed[1]	U	2.0	m s^{-1}
Production			
energy for fat deposition[4]	E_{fat}	51.75	MJ kg^{-1}
energy for protein deposition[4]	E_{prot}	32.13	MJ kg^{-1}
target body mass fraction for fat[4]	ρ_{fat}	0.15	nd
target body mass fraction for protein[4]	ρ_{prot}	0.267	nd
deposition efficiency for fat[4]	η_{fat}	0.76	nd
deposition efficiency for protein[4]	η_{prot}	0.56	nd
energy fraction derived from fat[5]	γ_{fat}	0.8335	nd

Figures

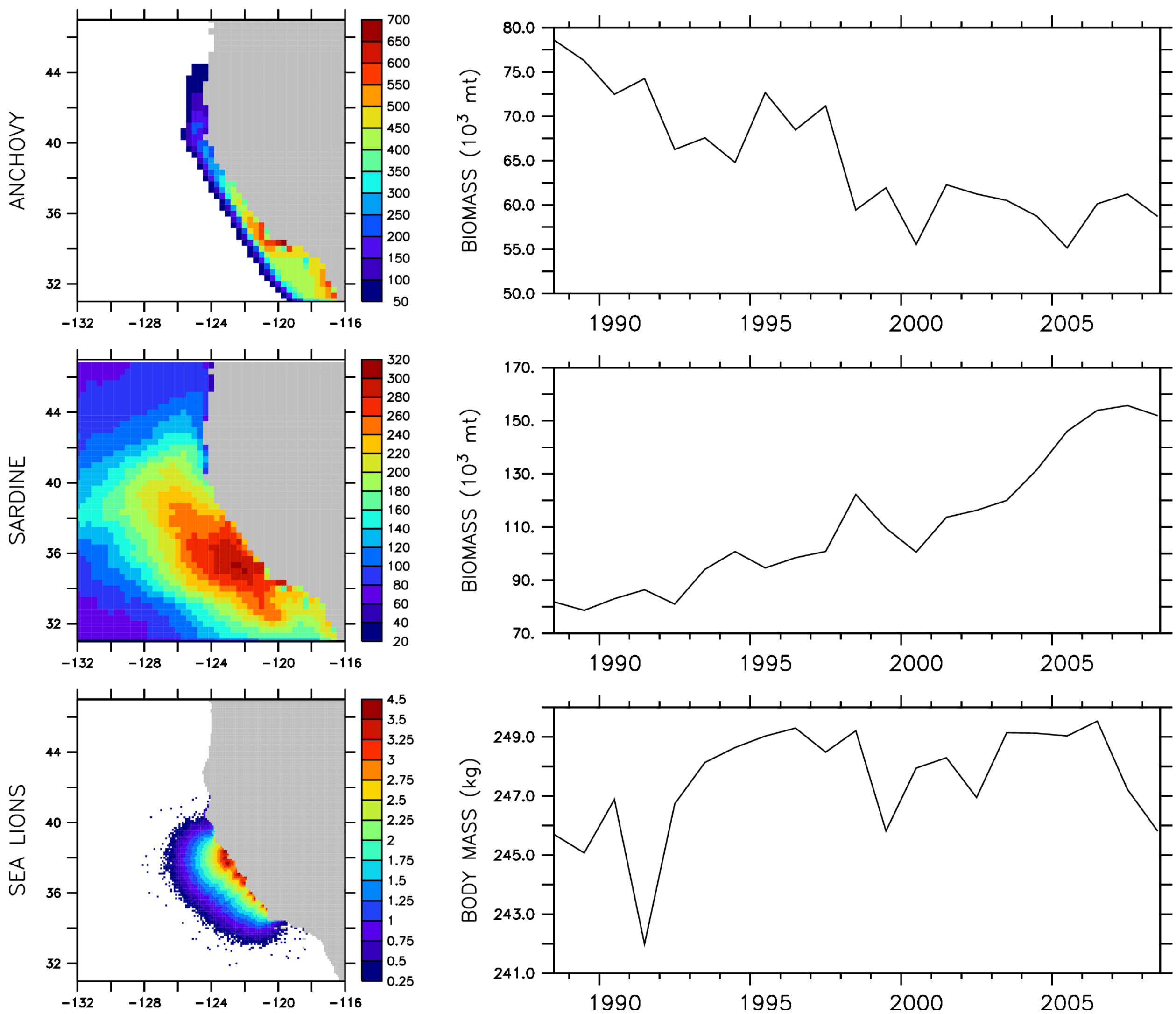

Figure S1. Simulated anchovy, sardine and sea lion population abundances during 1989-2008. Top: 20-year mean spatial distribution (left) and temporal variability (right) for adult anchovy abundance (millions of individuals). Middle: 20-year mean spatial distribution (left) and temporal variability (right) for adult sardine abundance (millions of individuals). Bottom: mean spatial distribution ($\log_{10}$[individuals]) (left) and temporal variability in sea lion population mean body mass (kg).

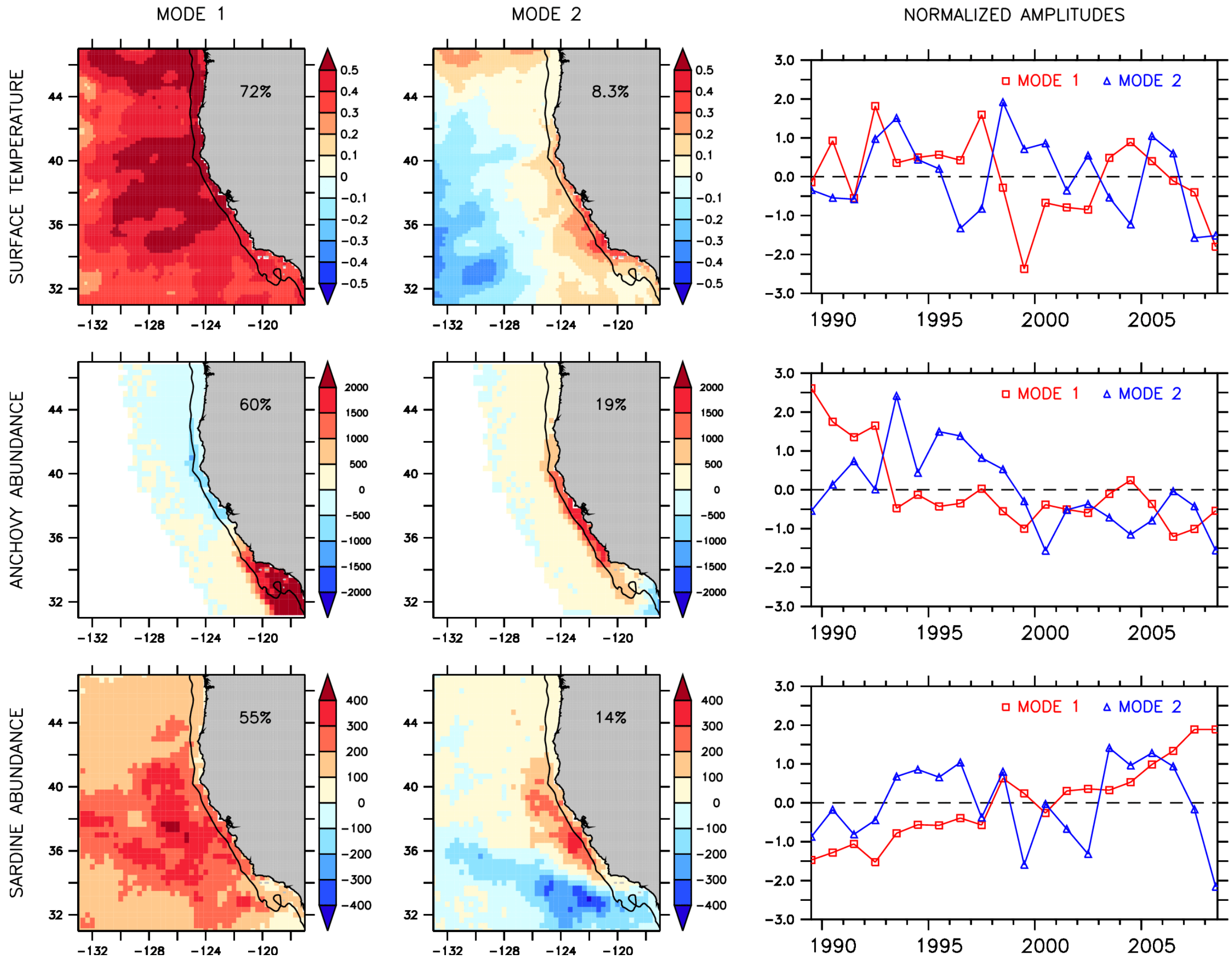

Figure S2. First (left) and second (center) EOF modes (with percent variance explained) and normalized annual amplitudes (right) for sea surface temperature (top), anchovy abundance (middle), and sardine abundance (bottom). Color scales denote temperature (°C) in top panels, and abundance (millions of individuals) in middle and bottom panels.

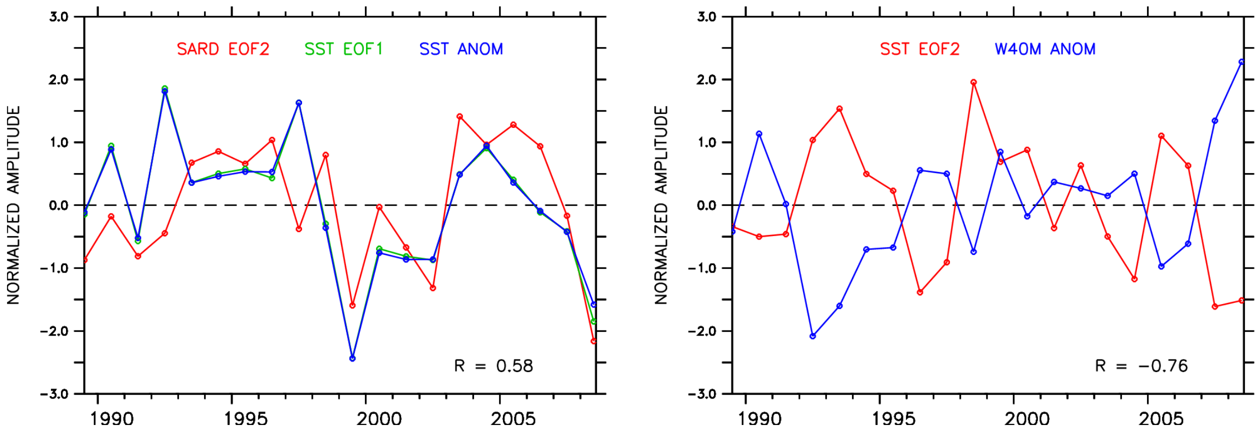

Figure S3. Relationships between environmental variability and explanatory EOFs for sea lion abundances. Left: correlation between simulated EOF mode 2 for sardine abundance, EOF mode 1 for SST, and spatially-averaged SST anomaly (normalized by standard deviation). Right: correlation between simulated EOF mode 2 for SST and mean vertical velocity (i.e., upwelling transport) at 40-m depth off of central California (averaged between 35 and 39°N and out to the 1000-m isobath).

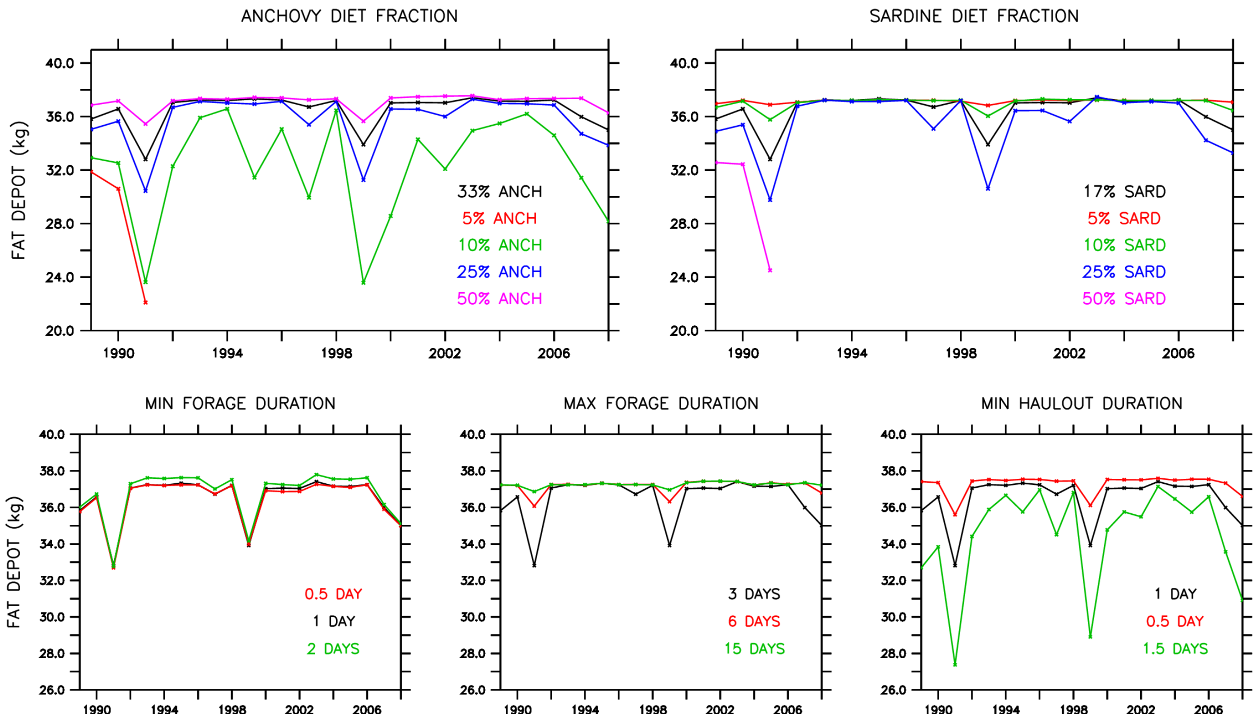

Figure S4. Sensitivity of sea lion simulated fat depot (kg) to diet composition (top) and model parameters (bottom) for 1989-2008. Top left: impact of anchovy diet fraction around a baseline value of 33% for a fixed sardine diet contribution of 17%. Top right: impact of sardine diet fraction around a baseline value of 17% for a fixed anchovy diet contribution of 33%. Bottom: impact of imposed minimum foraging duration (left), maximum foraging duration (center), and minimum haul-out duration (right).

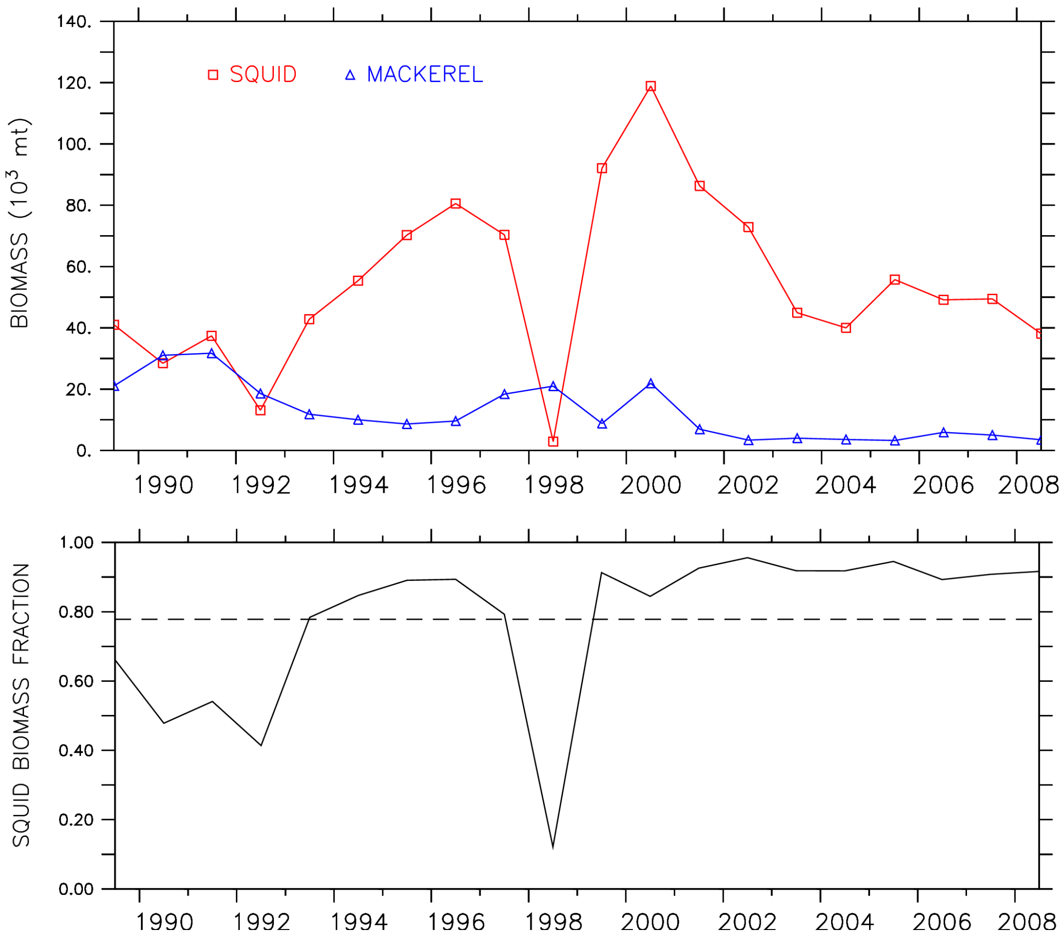

Figure S5. Relative abundance of market squid and jack mackerel during 1989-2008. Top: squid (red squares) and mackerel (blue triangles) biomass (10^3 mt) from California commercial catch data (PFMC, 2014). Bottom: fraction biomass of squid with respect to the total biomass of squid plus mackerel; the dashed line denotes the 1989-2008 mean squid biomass fraction (0.77).

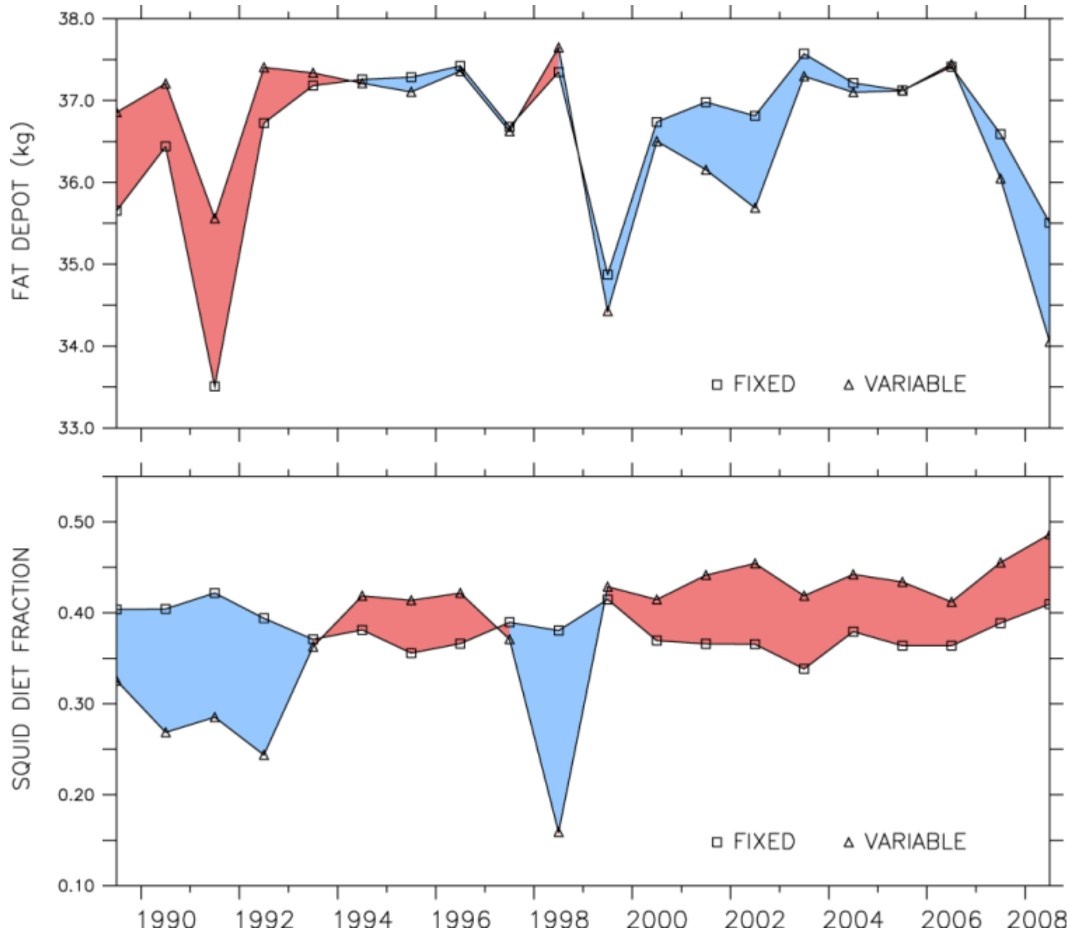

Figure S6. Sensitivity to prey assemblage. Top: annual mean fat depot (kg) where shading indicates periods during which a variable mackerel-to-squid ratio (triangles) yields lower (blue) and higher (red) fat depot than a fixed ratio (squares). Bottom: annual mean fraction of market squid in the sea lion diet where shading indicates periods during which squid consumption with a variable mackerel-to-squid ratio (triangles) is lower (blue) and higher (red) than with a fixed ratio (squares).